DOI: https://doi.org/10.37434/tpwj2023.07.04

INFLUENCE OF ELECTRON BEAM FOCUSING CURRENT ON GEOMETRY AND MICROSTRUCTURE OF WELDED JOINTS OF ALUMINIUM 2219 ALLOY

M.O. Rusynyk[1], V.M. Nesterenkov[1], M. Sahul[2], I.M. Klochkov[1]

[1]E.O. Paton Electric Welding Institute of the NASU
11 Kazymyr Malevych Str., 031 %0, Kyiv, Ukraine
[2]Czech Technical University in Prague, Faculty of Mechanical Engineering
Technicka 4, 160 00 Prague 6, Czech Republic

ABSTRACT

The influence of the focusing current of electron beam welding on the nature of the formation of welded joints of aluminium 2219 alloy was investigated. It was established that when the focusing current increases, the width of the face weld grows. And the width of the weld root depends on the real position of the electron beam focus relative to a sharp focus on the metal surface (639 mA). Dependence of the focusing current on the distribution of copper and aluminium in the weld metal was revealed. An increase in the focusing current from 629 to 649 mA led to an increase in the copper content in the interdendritic regions. Energy dispersion X-ray analysis showed that the microstructure of the welded joint produced at the focusing current of 629 mA, consists of equiaxial dendrites with embedded small particles, pores and α+θ-Al_2Cu eutectic, separated in the interdendritic regions.

KEYWORDS: electron beam welding, assembly and welding equipment, aluminium alloy, energy dispersive X-ray spectroscopy, segregation

INTRODUCTION

Aluminium 2219 alloy is a high-strength alloy consisting of aluminium, copper and manganese, which combines good treatment ability and qualitative mechanical properties. Products of this alloy can be used in the temperature range from –270 to 300 °C. At the same time, the alloy has higher mechanical properties compared to wrought alloys of the Al–Mg alloying system [1]. This alloy is a light metallic material with several desirable properties: low density, high specific strength and rigidity. Therefore, it is widely used in automotive, aircraft, aerospace and other industries that require lightweight structures [2]. The use of 2219 alloy became particularly widespread in the aerospace industry, namely, in the manufacture of rocket bodies, fuel tanks, chassis elements and other structural assemblies.

In welding alloys of the Al–Cu–Mg system, difficulties are caused by a great susceptibility of the weld metal to the formation of pores and crystallization cracks (especially typical for alloys based on aluminium). In welding alloys of an increased strength, cold cracking is observed. A significant shrinkage during weld crystallization, as well as high linear expansion coefficient lead to considerable residual deformations. In welding of hardened aluminium and thermally strengthened aluminium alloys, the strength of the welded joint is reduced compared to the strength of the base metal, which creates certain problems. Significant difficulties arise as a result of light oxidation of aluminium in solid and molten states. The formed refractory film of aluminium Al_2O_3 oxide hinders the weld formation and it is a source of nonmetallic inclusions in the weld metal.

Electron beam welding (EBW) compared to other types of welding these types of alloys has several advantages. The welding process runs in vacuum, which is important for chemically active alloys. It is also featured by a quick process of heating and cooling of the metal, which in turn determines the minimal softening of welded joints, and the maximum level of their strength properties. Temporary inner stresses do not have time to affect the solidified metal, i.e., crystallization cracks have no time to arise. For high-strength aluminium alloys, it is possible to avoid metal softening in the near-weld zone at high welding speeds that provide minimal thermal influence on the base metal [3]. The use of EBW allowed reducing the volume of molten metal of the weld pool and dimensions of the heat-affected zone (HAZ) and this led to a decrease in the rate of growth of elastic-plastic deformations in the temperature range of brittleness and an increase in the margin of technological strength of material to be welded [4, 5].

To produce welded joints with the required properties, it is necessary to optimize EBW parameters. The focusing current is one of the main EBW parameters, which affects the focus position and, thus, the total power density created by the electron beam on

Table 1. Chemical composition of plates of 2219 alloy, wt.%

Al	Cu	Mn	V	Fe	Si	Zn	Zr	Ti
Base	6.23	0.32	0.09	0.13	0.28	0.03	0.1	0.07

the surface of the materials to be welded. Until now, there is no information on the study of the influence of the focusing current on the microstructure and the mechanical properties of AA2219 alloy welded by electron beam. Only individual authors investigated the influence of the focus position and the angle of incidence of the beam on the behaviour of the molten pool in the welding AA2219 alloy. It was found that the smallest porosity in the welds of AA2219 alloy was observed when the focus was applied by 8 mm lower than the surface of the metal to be welded [6]. At the moment, other results of studying the alloy, considered in the work, are unknown. The studies and obtained results are unique and contribute to explaining the influence of the focusing current on the geometry and microstructure of welded joints of aluminium 2219 alloy.

The aim of this work is to investigate the effect of the EBW focusing current on the geometry and microstructure of welded joints of aluminium 2219 alloy at a constant input energy of welding and accelerating voltage.

PROCEDURE OF WORK PERFORMANCE

For the study, the plates of aluminium 2219 alloy of 10 mm thickness were used.

The chemical composition of the base material of aluminium 2219 alloy was measured using the X-ray fluorescence spectroscopy. For measurements, the portable X-ray Delta line analyzer of the Innov-X Company was used. The chemical composition was measured in three different places and average values were calculated. XRF results are given in Table 1. A small amount of zirconium (0.1 wt.%) causes a change in grain, namely, reduces the grain size of the alloy.

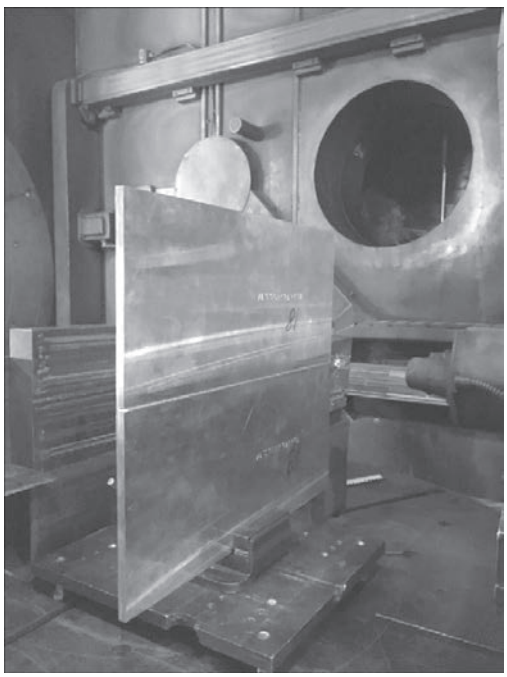

Figure 1. Scheme of EBW using horizontal beam in a horizontal plane

The point EDS analysis of a local chemical composition was performed in an equiaxial zone near the penetration boundary for welded joints produced during focusing currents of 629 and 649 mA.

The chemical composition was analyzed using the energy dispersive X-ray spectroscopy method (EDS): JEOL 7600F SEM FEG with X-max 50 mm^2 analyzer of the Oxford Instruments Company.

The welding process took place in an electron beam welding installation of UL-209M type.

The configuration of the installation involves a movable intrachamber welding gun with a computer numerical control (CNC) for movement of a cantilever type. This mechanism provides a linear movement along the three Cartesian coordinate axes (along the chamber — *X*, across — *Y* and vertical — *Z*), as well as the inclination of the gun at an angle of 90° in the *Z–X* plane (from the "vertical" position of the gun to the "horizontal"). In this case, this "inclination" is performed by rotating the entire cantilever beam, which is the base of the mechanism for movement along the *Y* axis. The beam itself can move freely in the *Z–X* plane within most dimensions of the welding chamber.

The welding gun unit can have an additional degree of freedom — rotation axis of the gun in a plane parallel to the *Y* axis — usually at ± 45° (i.e., axis of this rotation is perpendicular to the *Y* axis).

The installations of this type are completed with a high-voltage welding source with a capacity of 15 %, 30 or 60 kW (at an accelerating voltage of 60 kV) depending on the specific materials to be welded and their thickness.

For welding of plates of different sizes, assembly and welding equipment was developed, in which a batch of butt joints with a through penetration at different welding parameters was welded.

It is known that due to a high thermal conductivity of aluminium, special requirements are specified to the types of welded joints. The uniform weld formation is achieved only at a symmetrical arrangement of the heating source relative to welded edges. At the same time, the scheme of EBW using the horizontal beam in the horizontal plane was chosen (Figure 1). Such an arrangement of the welding pool facilitates the degassing of a liquid metal and its refinement,

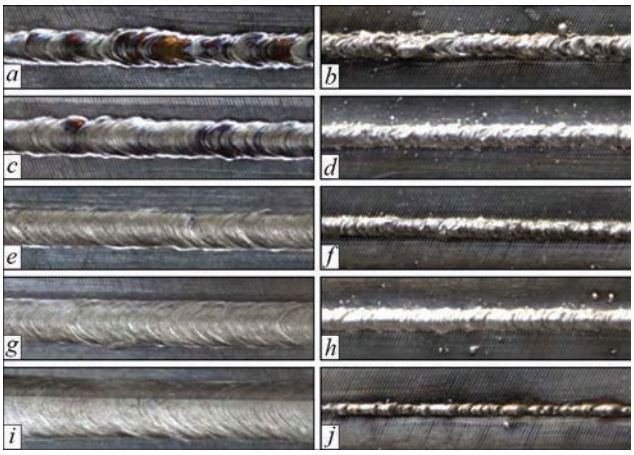

Figure 2. Face and root appearance of welds produced at different values of focusing current, mA: *a*, *b* — 629; *c*, *d* — 634; *e*, *f* — 639 — acute focus; *g*, *h* — 644; *i*, *j* — 649

Table 2. Parameters of welding plates of 2219 alloy

Specimen	Welding current, mA	Welding speed, mm/s	Acceleration voltage, kV	Focusing current, mA	Input energy, J/mm
1	85	20	60	629	255
2				634	
3				639	
4				644	
5				649	

which in turn reduces the requirements for cleanliness and quality of preparation of surfaces to be joined.

RESEARCH RESULTS

At the first stage, the effect of the focusing current on the shape and geometry of the welds was considered. For this purpose, the following welding modes were selected (Table 2). On these modes, plates of 2219 alloy were welded.

Welding was carried out with different focusing currents (Table 2), namely: 629, 634, 639, 644 and 649 mA, where the value of 639 mA is a sharp focus, i.e., the focusing current is on the surface of the plate to be welded (Figure 2, e, f). For the study, welds with the minimum 629 mA and the maximum of 649 mA focusing currents were selected. Other parameters (welding current, welding speed, etc.) were not changed.

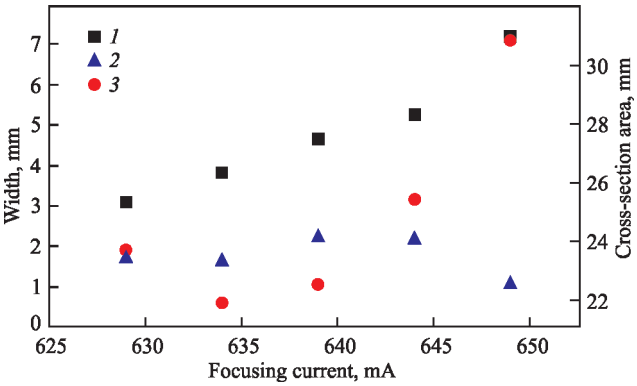

Figure 4. Dependence of the width of face weld (*1*), weld root (*2*) and cross-section area (3) on the value of focusing current

Figure 3 shows cross-sections of the welds produced on different focusing currents. According to this picture, it is possible to evaluate the proportionality of the width of the weld to its length.

The measurements showed that the growth of the width of the facial part of the weld is directly proportional to the growth of the focusing current. However, it is impossible to state this regarding the root. At smaller values of the focusing current, the root width is smaller than at acute focus. But already at much larger values of the focusing current, the width of the root decreases (Figure 4).

To analyze the microstructure of welds, the methods of scanning electron microscopy (SEM) and energy dispersive X-ray spectroscope (EDS) were used.

The microstructure of the base metal of aluminium AA2219 alloy is presented in Figure 5. The alloy microstructure consists of elongated grains of a solid aluminium solution (α); tiny and coarse bright particles distributed mainly on grain boundaries. In the image obtained with the help of backscattered electrons (BSE), a significant difference in brightness between the particles and matrix indicates the presence of heavy elements. According to the chemical composition of the base metal, copper is considered to be this element. In addition, the presence of copper was confirmed by quantitative and qualitative EDS analysis.

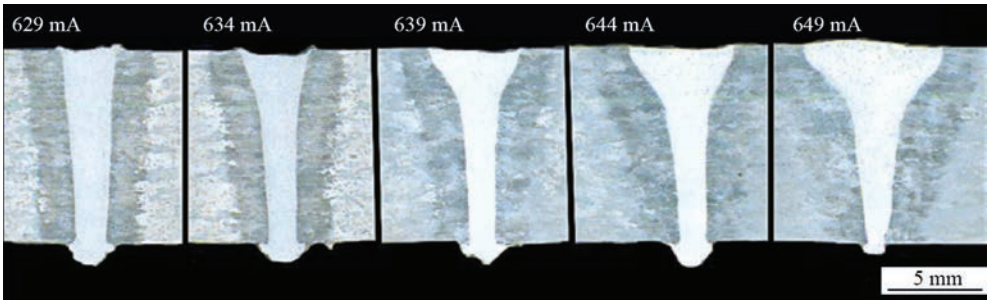

Figure 3. Influence of focusing current on welds geometry

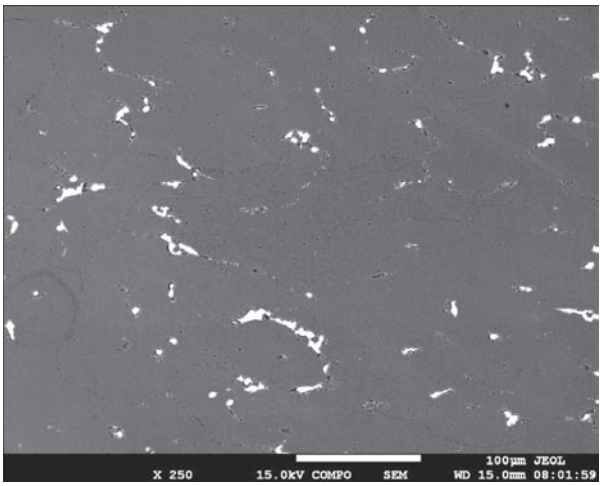

Figure 5. Microstructure of base metal of 2219 alloy

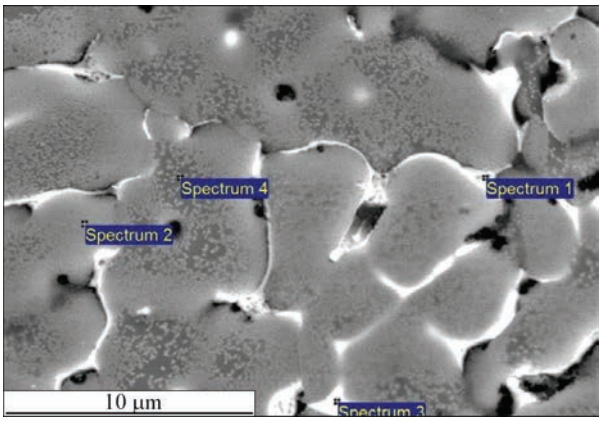

Figure 6. Microstructure of weld metal (focusing current is 629 mA)

Microstructure of the welded joint produced at a focusing current of 629 mA consists of equiaxial dendrites with embedded tiny particles, pores and α + θ Al_2Cu eutectics, separated in the interdendritic regions (Figure 6). The local elemental composition, which was measured from four regions (Spectra 1–4) is given in Table 3. Spectra 1 and 3 were obtained from the interidendritic regions, enriched by separated alloying elements. Compared to dendrites, these zones look brighter and contain about 14 at.% of copper. Accord-

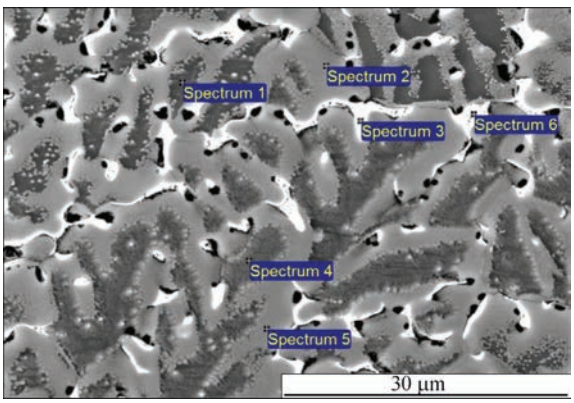

Figure 7. Microstructure of weld metal (focusing current is 649 mA)

Table 3. Chemical composition of weld metal according to EDS analysis (focusing current is 629 mA) (at.%)

Spectra	O	Al	Mn	Fe	Cu
1	6.05	79.43	0.14	0.27	14.10
2	2.65	93.72	0.17	–	3.46
3	3.21	82.15	0.22	0.37	14.06
4	3.15	95.40	0.13	–	1.32

Table 4. Chemical composition of weld metal according to EDS analysis (focusing current is 649 mA) (at.%)

Spectra	O	Al	Mn	Fe	Cu
1	2.00	96.78	0.14	–	1.08
2	0.37	94.91	0.13	–	4.59
3	7.90	71.96	0.14	0.33	19.67
4	2.74	95.57	0.15	–	1.54
5	0.57	94.57	0.18	–	4.67
6	3.95	72.86	0.11	0.31	22.79

ing to the binary diagram aluminium-copper, eutectic may be identified, containing α(Al) + θ(Al_2Cu). In Spectrum 2, a decrease in the copper content and an increase in the aluminium content were observed. The aluminium content revealed in Spectrum 2, amounted to 93.7 at.%. The highest amount of aluminium was measured in the region marked as Spectrum 4, where 95.4 at.% of aluminium was detected.

According to the binary phase Al–Cu diagram, at a homogeneous crystallization, the alloy contains about 2.36 % of α(Al) + θ(Al_2Cu) eutectics. However, the process of crystallization during welding is usually heterogeneous. This leads to the microsegregation of Cu. Therefore, the amount of eutectics in the welded joint is higher than 2.36 %, and the content of Cu in the matrix α(A1) is lower than 5.65 % [7].

The EDS analysis conducted in the weld metal with the focusing current of 629 mA relative to the selected regions is shown in Table 3.

Microstructure of the welded joint produced at a focusing current of 649 mA is shown in Figure 7 and Table 4. The dendritic microstructure was formed after crystallization of the melt pool. The local chemical composition was measured in Spectra 1-6. Spectra 1 and 4 represented dendrites with a high aluminium content. Thus, in these spectra, more than 95 at.% of aluminium were measured in these spectra. In this case, a solid aluminium solution was recorded. An increase in the copper content was observed in Spectra 2 and 5. On the image of backscattered electrons, these places were slightly brighter compared to previous ones. The copper content, which was observed in these places, amounted to 4.6 and 4.7 at.%, respectively. The brightest zones in the deposited metal were observed in Spectra 3 and 6. In such places, a significant increase in the copper content was observed. On

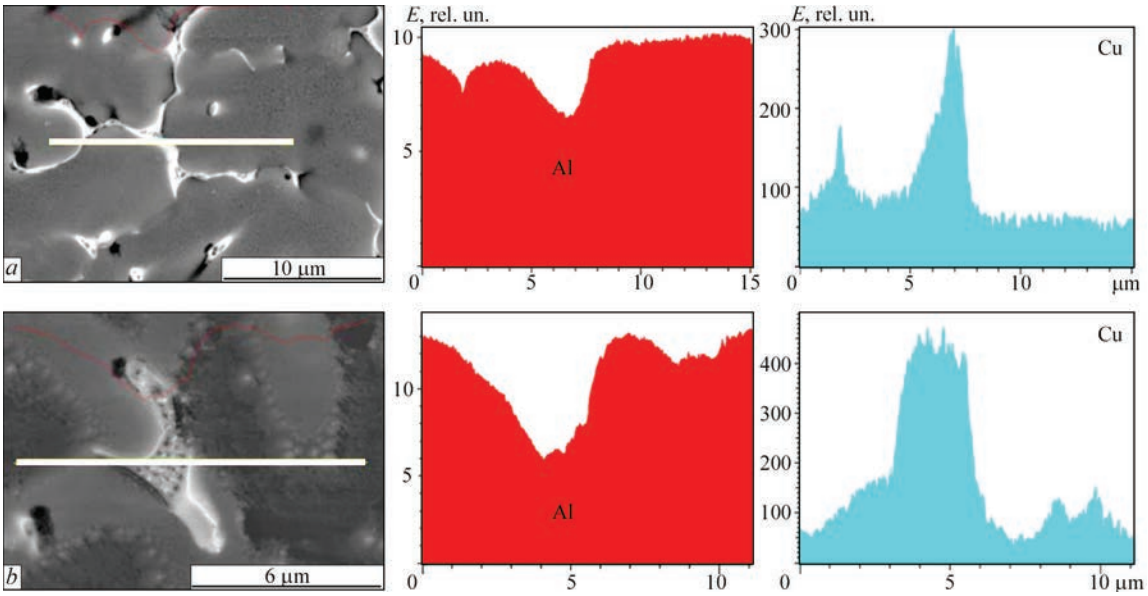

Figure 8. Linear EDS scanning through dendritic zones, in the metal of welds produced using focusing current: *a* — 629; *b* — 649 mA

the other hand, the drop of aluminium content was observed in the abovementioned Spectra 3 and 6. Spectrum 3 was characterized by the content of about 19.7 at.% of copper. In Spectrum 6, 22.8 at.% of copper was revealed. This is associated with the segregation, when interdendritic regions are enriched with alloying elements, in our case, it is mostly copper. The eutectics consisting of $\alpha(Al) + \theta(Al_2Cu)$ can be highlighted in this place, as it follows from the abovementioned binary diagram. In addition, in Spectra 3 and 6, iron was also recorded.

A high cooling rate, characteristic of EBW, not only contributes to the microsegregation, but also improves the solubility of Cu in Al, which is usually lower than 2 % in the conditions of a uniform crystallization process. In addition, it was found [8], that if the current increases, more copper amount diffuses into a solid substance. According to our observations, an increase in the focusing current from 629 to 649 mA has led to an increase in Cu content in the interdendritic regions. However, with the higher Cu content on the grain boundaries, the sensitivity to hot cracking can increase significantly.

Linear EDS scanning along the interdendritic regions were carried out in the metal of welds produced using focusing currents of 629 (Figure 8, *a*) and 649 mA (Figure 8, *b*). The placement of aluminium and copper was observed across the white lines given in (Figure 8, *a*, *b*). In the interdendritic region, a clear increase in Cu and a sharp decrease in Al were recorded. This phenomenon is associated with the presence of microsegregated eutectics in the interdendritic regions. The presence of eutectics was also confirmed by local quantitative EDS analysis.

CONCLUSIONS

1. The influence of the current focusing of electron beam welding on the formation of welds of aluminium 2219 alloy for the plates of up to 20 mm thickness was investigated. It was established that with an increase in the focusing current, the width of the face weld grows. In turn, the width of the weld root depends more on the real position of the focus of the electron beam relative to a sharp focus (639 mA).

2. The dependence of the focusing current on the distribution of copper and aluminium in the weld metal was revealed. An increase in the focusing current from 629 to 649 mA has led to an increase in the content of copper in the phase precipitates placed in the interdendritic regions. An increase in the copper content led to the formation of eutectics in the mentioned interdendritic regions. In the regions of the spectra, where a decrease in the aluminium content was recorded, also an increase in the copper content was observed, associated with segregation.

3. With the help of the energy dispersion X-ray analysis, the microstructure of the weld metal at different focusing currents was determined. Thus, coarser dendrites are formed at the expansion of the weld, which in the tested range of beam focusing corresponds to the higher value of the focusing current.

4. The local quantitative EDS analysis confirmed the presence of $\alpha + \theta(Al_2Cu)$ eutectics in the interdendritic regions of the weld metal.

REFERENCES

1. Vinogradova, N.M., Starostina, Z.I., Ivanova, T.V. (1975) Aluminium weldable alloys 1201 and 01381 for operation at low temperatures. *Aluminium Alloys,* **7**, 65–71 [in Russian].

2. Heinz, A., Haszler, A., Keidel, C. et al. (2000) Recent development in aluminum alloys for aerospace application. *Mater. Sci. Eng.*, **280**, 102–107.
3. Skalskyi, V.P., Andreikiv, O.Ie. (2006) *Evaluation of bulk damage of materials by acoustic emission method.* Lviv, Vydavn. Tsentr Nats. Un-tu [in Ukrainian].
4. Ternovoj, E.G., Bondarev, A.A. (2012) Electron beam welding of aluminium AMg6 and M40 alloys. *The Paton Welding J.,* **4**, 8–14.
5. Bondarev, A.A. (1984) State-of-the-art and advantages of electron beam welding process of aluminium alloy structures. In: *Proc. of Soviet-American Seminar on Welding of Aluminium Alloys of Cryogenic and General Purpose.* Kyiv, 10–19.
6. Yang, Z., He, J. (2021) Numerical investigation on fluid transport phenomena in electron beam welding of aluminum alloy: Effect of the focus position and incident beam angle on the molten pool behavior. *Int. J. Therm. Sci.* **164**, 106914. DOI: https://doi.org/10.1016/j.ijthermalsci.2021.106914
7. Quan, Li, Ai-ping, Wu, Yan-jun,Li, et al. (2017) Segregation in fusion weld of 2219 aluminum alloy and its influence on mechanical properties of weld. *Transact. of Nonferrous Metals Society of China*, 27(**2**), 258–271. DOI: https://doi.org/10.1016/S1003-6326(17)60030-X
8. Ruwei, Geng, Jun, Du, Zhengying, Wei et al. (2020) Multiscale modelling of microstructure, micro-segregation, and local mechanical properties of Al–Cu alloys in wire and arc additive manufacturing. *Additive Manufacturing*, **36**, 101735. DOI: https://doi.org/10.1016/j.addma.2020.101735
9. Poklyatskyi, A.G., Motrunich, S.I., Klochkov, I.M., Labur, T.M. (2021) Some advantages of welded joints of aluminium 1201 alloy produced by friction stir welding. *The Paton Welding J.,* **9**, 15–19. DOI: https://doi.org/10.37434/tpwj2021.09.03

ORCID
M.O. Rusynyk: 0000-0002-7591-7169,
V.M. Nesterenkov: 0000-0002-7973-1986,
I.M. Klochkov: 0000-0001-6490-8905

CONFLICT OF INTEREST
The Authors declare no conflict of interest

CORRESPONDING AUTHOR
V.M. Nesterenkov
E.O. Paton Electric Welding Institute of the NASU
11 Kazymyr Malevych Str., 03150, Kyiv, Ukraine.
E-mail: nesterenkov@technobeam.com.ua

SUGGESTED CITATION
M.O. Rusynyk, V.M. Nesterenkov, M. Sahul, I.M. Klochkov (2023) Influence of electron beam focusing current on geometry and microstructure of welded joints of aluminium 2219 alloy. *The Paton Welding J.*, **7**, 31–36.

JOURNAL HOME PAGE
https://patonpublishinghouse.com/eng/journals/tpwj

Received: 25.05.2023
Accepted: 06.09.2023